

Stagnation point flow and heat transfer over a non-isothermal permeable stretching sheet

K. Swain¹, J.P.Tripathy²

¹Department of Mathematics, Gandhi Institute For Technology, Bhubaneswar, Odisha-752054, India

²Gandhi Engineering College, BBSR, Odisha

Abstract: The present study intend to analyze the simultaneous effect of heat and mass transfer on boundary layer stagnation point flow of a viscous fluid over a non-isothermal stretching sheet subject to transverse magnetic field and variable surface temperature. The flow medium is considered to be porous. The governing partial differential equations (PDEs) are converted into ordinary differential equations (ODEs) by suitable similarity transformations. The numerical simulation is carried out by using Runge-Kutta method of fourth order with shooting technique. The physical significance of pertinent parameters of the flow phenomenon are studied through graphs and tables. Moreover, skin friction coefficient, Nusselt number and Sherwood number are computed and analysed in details.

Keywords: Stretching sheet, stagnation point, thermal radiation, porous medium.

I. Introduction

The boundary layer flow over a stretching/shrinking surface is an important engineering and practical applications in manufacturing such as extrusion process, cooling of metallic sheets or electric chips, paper production, glass fiber, glass blowing, drawing plastic film, metal spinning etc. The nature of the final products depend on the heat and mass transfer rate between the variable stretching or shrinking surface with variable temperature. Crane [1] was first discussed the boundary layer flow over a linearly stretching surface. Several extensional work over a stretching sheet using different flow models are

Nomenclature

B_0	Magnetic field strength	T_∞	Ambient temperature (K)
C	Concentration of the solute (kg/m ³)	T_w	Wall temperature (K)
C_∞	Ambient concentration (kg/m ³)	u, v	Velocity components in x- and y-directions respectively (m/s)
C_w	Wall concentration (kg/m ³)	Greek symbols	
c_p	Specific heat (J/kg.K)	α	Thermal diffusivity (m ² /s)
D	Diffusion coefficient (m ² /s)	ε	Velocity ratio parameter
g	Acceleration due to gravity	β	Thermal expansion coefficient
Gr_x	Thermal Grashof number	β^*	Concentration expansion coefficient
Gc_x	Solutal Grashof number	η	Dimensionless variable
k	Thermal conductivity of the fluid (W/m.K)	ρc_p	Specific heat capacitance of the fluid (J/kg.K)
k^*	Mean absorption coefficient	ρ	Density of the fluid (kg/m ³)
K^*	Permeable parameter	ν	Kinematic viscosity of the fluid (m ² /s)
K	Porosity parameter	μ	Dynamic viscosity of the fluid (kg/m.s)
M	Magnetic parameter	ψ	Stream function (m ² /s)
m, n	power-law exponents	θ	Dimensionless temperature
Pr	Prandtl number	ϕ	Dimensionless concentration
q_r	Radiative heat flux (W/m)	σ	Electrical conductivity of the fluid (S/m)
R	Radiation parameter	σ^*	Stefan-Boltzman constant (W/m ² .K ⁴)
S	Suction/injection parameter	λ_1	Thermal buoyancy parameter
Sc	Schmidt number	λ_2	Solutal buoyancy parameter
T	Temperature of the fluid (K)		

discussed by many authors [2-4]. Stagnation point is a point where the motion of fluid particles is zero corresponding to the body. Stagnation point occurs at the surface of a body in the flow distribution, where the fluid is forced to rest by the body. Layek et al. [5] discussed a similarity analysis to study the heat transfer effects on stagnation point flow along a stretching surface embedded in a porous medium with suction/blowing and heat absorption/generation. Bhattacharya [6] analysed the dual solution for boundary layer stagnation point flow over a shrinking/stretching surface. The influence of mass and heat transfer over MHD mixed convection stagnation point flow along with a vertical sheet attached with a highly permeable medium having radiation and internally heat generation has investigated by Makinde [7]. Ishak et al. [8] studied behavior of fluid past along a stretching surface due to MHD stagnation point flow. Moreover, the heat transfer phenomenon of MHD stagnation point flow of nanofluid past a stretching surface has been discussed by Ibrahim [9]. The study of two dimensional stagnation point flow of an incompressible conducting fluid with variable fluid properties in porous medium is carried out by Swain et.al [10]. Khan et. al [11] discussed the impact of MHD on stagnation point movement on a nonlinear oscillating plate in the presence of slip boundary conditions.

Motivated by the above literature and to the best of authors' knowledge, there is no investigation has been carried out which deliberates the combined effects of heat and mass transfer phenomenon on stagnation point flow an electrical conducting fluid due to the applied uniform transverse magnetic field along a permeable non-isothermal shrinking surface. The study also takes care of variable surface temperature, thermal radiation and mass suction/injection. The governing PDEs are converted to nonlinear ODEs by the help of similarity transformations. The numerical solutions of self-similar ODEs with the prescribed boundary conditions are solved by using the Runge-Kutta method of fourth order with shooting technique. To study the behavior of pertinent physical parameters on the velocity, temperature and concentration distributions, graphs and tables are plotted and discussed in details.

II. Mathematical analysis of the problem

Consider a steady, laminar, two dimensional, incompressible and electrically conducting viscous fluid flow near a stagnation point over a non-isothermal permeable stretching sheet embedded in a saturated porous medium. The flow is subjected to a constant transverse magnetic field of strength B_0 is applied along y-axis, normal to the sheet. The effects of thermal and mass buoyancy with thermal radiation are also considered. Using the boundary layer approximation, the governing equations of continuity, momentum, energy and concentration are expressed as:

$$u \frac{\partial u}{\partial x} + v \frac{\partial v}{\partial y} = 0, \tag{1}$$

$$u \frac{\partial u}{\partial x} + v \frac{\partial u}{\partial y} = U_s \frac{dU_s}{dx} + \nu \frac{\partial^2 u}{\partial y^2} - \frac{\sigma B_0^2}{\rho} u + g\beta(T - T_\infty) + g\beta^*(C - C_\infty) - \frac{\nu u}{K^*}, \tag{2}$$

$$u \frac{\partial T}{\partial x} + v \frac{\partial T}{\partial y} = \frac{k}{\rho c_p} \frac{\partial^2 T}{\partial y^2} - \frac{1}{\rho c_p} \frac{\partial q_r}{\partial y}, \tag{3}$$

$$u \frac{\partial C}{\partial x} + v \frac{\partial C}{\partial y} = D \frac{\partial^2 C}{\partial y^2}. \tag{4}$$

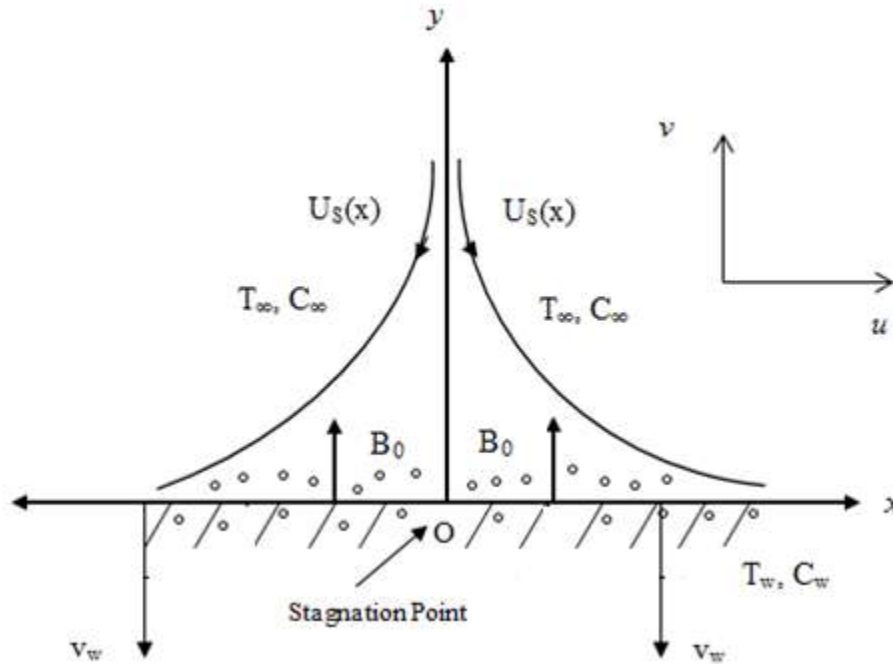


Fig. 1 Flow geometry and coordinate system

The prescribed boundary conditions are

$$\left. \begin{aligned} u = U_w(x) = cx, v = v_w, T = T_w = T_\infty + T_0 x^n, C = C_w = C_\infty + C_0 x^m & \text{ at } y = 0 \\ u \rightarrow u(x) = ax, T \rightarrow T_\infty, C \rightarrow C_\infty & \text{ as } y \rightarrow \infty \end{aligned} \right\} \quad (5)$$

Here U_w is the shrinking velocity, $c < 0$ stands for shrinking rate ($c > 0$ for stretching rate) and $a > 0$ is the strength of the stagnation flow, T_∞ is the constant free stream temperature, T_w is the wall temperature, T_0 is a constant depends upon the thermal properties of the fluid, C_∞ is the constant free stream concentration, C_w is the wall concentration and C_0 is a constant depends upon the mass properties of the fluid and m, n are power-law exponents, $v_w > 0$ refers to suction velocity and $v_w < 0$ refers to injection velocity.

The stream function $\psi(x, y)$ is defined as

$$u = \frac{\partial \psi}{\partial y} \quad \text{and} \quad v = -\frac{\partial \psi}{\partial x} \quad (6)$$

Using Rosseland approximation (Swain et al. [12]), the radiative heat flux is given by

$$q_r = \frac{-4\sigma^*}{3k^*} \frac{\partial T^4}{\partial y} \quad (7)$$

where σ^* is the mean absorption coefficient and k^* is the Stefan-Boltzmann constant. It is taken care that the temperature difference within the flow, such as the expression T^4 may be presented as a function of temperature. We have the Taylor series expansion for T^4 at a free stream temperature T_∞ and after neglecting high order term we approximate $T^4 = 4T_\infty^3 T - 3T_\infty^4$

From the above relation (7), we have

$$\frac{\partial q_r}{\partial y} = \frac{-16\sigma^* T_\infty^3}{3k^*} \frac{\partial^2 T}{\partial y^2} \quad (8)$$

Hence, equation (3) becomes

$$u \frac{\partial T}{\partial x} + v \frac{\partial T}{\partial y} = \frac{1}{\rho c_p} \left(k + \frac{16\sigma^* T_\infty^3}{3k^*} \right) \frac{\partial^2 T}{\partial y^2}, \quad (9)$$

Consider the following transformations

$$\psi = \sqrt{av}xf(\eta), T = T_\infty + (T_w - T_\infty)\theta(\eta), C = C_\infty + (C_w - C_\infty)\phi(\eta), \quad (10)$$

and the similarity variable η can be expressed as $\eta = y\sqrt{\frac{a}{\nu}}$.

In view of equation (10), the equation (1) is identically satisfied and the equations (2), (9), (4) and (5) reduce to

$$f''' + ff'' - (f')^2 + 1 - (M + K)f' + \lambda_1\theta + \lambda_2\phi = 0, \quad (11)$$

$$\left(1 + \frac{4}{3}R\right)\theta'' + \text{Pr}(f\theta' - n f'\theta) = 0, \quad (12)$$

$$\phi'' + Sc(f\phi' - m f'\phi) = 0, \quad (13)$$

$$\left. \begin{aligned} f(\eta) = S, f'(\eta) = \varepsilon, \phi(\eta) = 1, \theta(\eta) = 1 \text{ at } \eta = 0, \\ f'(\eta) \rightarrow 1, \theta(\eta) \rightarrow 0, \phi(\eta) \rightarrow 0 \text{ as } \eta \rightarrow \infty. \end{aligned} \right\} \quad (14)$$

Here prime denotes the differentiation with respect to η and $M = \frac{\sigma B_0^2}{\rho a}, K = \frac{K^* a}{\nu}$,

$$Gr_x = \frac{g\beta T_0 x^{n-1}}{\nu^2}, Gc_x = \frac{g\beta^* C_0 x^{m-1}}{\nu^2}, \text{Pr} = \frac{\mu c_p}{\alpha}, R = \frac{4\sigma^* T_\infty^3}{kk^*}, \lambda_1 = \frac{Gr_x}{\text{Re}_x^2}, \lambda_2 = \frac{Gc_x}{\text{Re}_x^2}, Sc = \frac{\nu}{D}, m, n$$

are power law exponents, $S = -\frac{v_w}{\sqrt{av}}$ where $S > 0$ (i.e. $v_w < 0$) refers to suction and $S < 0$ (i.e. $v_w > 0$)

refers to injection and $\varepsilon = \frac{c}{a}$.

III. Skin friction, Nusselt number and Sherwood number

The physical parameter of engineering interest concerning the thermal boundary layer are skin friction coefficient C_f , the local Nusselt number Nu_x and the local Sherwood number Sh_x which are defined as follows

$$C_f = \frac{\mu}{\rho_f u_w^2} \left(\frac{\partial u}{\partial y} \right)_{y=0} \quad (15)$$

$$Nu_x = \frac{-x}{(T_w - T_\infty)} \left[\frac{\partial T}{\partial y} - \frac{4\sigma^*}{3k^*} \left(\frac{\partial T^4}{\partial y} \right) \right]_{y=0} \quad (16)$$

$$Sh_x = \frac{-x}{(C_w - C_\infty)} \left(\frac{\partial C}{\partial y} \right)_{y=0} \quad (17)$$

The non-dimensional form of equations (15) – (17) are given by

$$\text{Re}_x^{0.5} C_f = f''(0) \quad (18)$$

$$\text{Re}_x^{-0.5} Nu_x = -\left(1 + \frac{4}{3}R\right)\theta'(0) \quad (19)$$

$$\text{Re}_x^{-0.5} Sh_x = -\phi'(0) \quad (20)$$

where $\text{Re}_x = \frac{u_w x}{\nu}$ is the local Reynolds number.

IV. Results and discussion

The system of non-linear coupled ODEs (11) – (13) with corresponding boundary conditions (14) are solved numerically by using Runge-Kutta method of fourth order with shooting technique. An investigation has been carried out to know the influence of various physical parameters such as magnetic parameter (M), porosity parameter (K), radiation parameter (R), Prandtl number (Pr), thermal buoyancy parameter (λ_1),

injection/suction parameter (S), velocity ratio parameter (ε), Schmidt number (Sc), mass buoyancy parameter (λ_2) on velocity, temperature, and concentration, graphs and tables are drawn. During numerical simulations the values of the parameters are fixed as $M = \lambda_1 = \lambda_2 = 1, K = 0.5, m = n = 2, R = \varepsilon = 0.1, Pr = 0.7$, and $Sc = 0.6$ unless otherwise specified. In order to validate our results, we are compared the results of $f''(0)$ and $\theta'(0)$ with Wang [13] and found them in excellent agreement, Table 1. Thus, the present results are more accurate than their results.

Table 1 Comparison of $f''(0)$ and $\theta'(0)$ for different values of ε when $M = K = \lambda_1 = \lambda_2 = R = S = 0$ and $Pr = n = 1$

ε	$f''(0)$		$\theta'(0)$	
	Wang [13]	Present study	Wang [13]	Present study
0	1.232588	1.2325876	-0.811301	-0.8113016
0.1	1.14656	1.1465610	-0.86345	-0.8634518
0.2	1.05113	1.0511300	-0.91330	-0.9133029
0.5	0.71330	0.7132949	-1.05239	-1.0514585
1	0	0	-1.25331	-1.2533142
2	-1.88731	-1.8873065	-1.58957	-1.5895673
5	-10.26475	-10.2647493	-2.33810	-2.3380991

From Table 3 it is perceived that rate of heat transfer declines with an increase in magnetic parameter, radiation parameter and Schmidt number while enhances with velocity ratio parameter, thermal and solutal buoyancy parameters. Further, velocity ratio parameter, thermal and solutal buoyancy parameters, radiation parameter and Schmidt number boost the mass transfer rate except magnetic parameter.

Table 3 Computation of $\theta'(0)$ and $\phi'(0)$ when $K = 0.5, S = 0.1, Pr = 0.6$ and $m = n = 2$

M	ε	λ_1	λ_2	R	Sc	$\theta'(0)$	$\phi'(0)$
0.1	0.1	1	1	0.1	0.6	1.0894726	1.1311380
0.5						0.9036256	0.8919633
1						0.8629699	0.8516097
	0.3					0.9463949	0.9331573
	0.5					1.0257644	1.0107668
		2				1.0645979	1.0491001
		5				1.2028032	1.2099112
			3			1.2226306	1.2225614
			5			1.2515259	1.2473065
				0.5		1.0500853	1.2532992
				1		0.8997379	1.2686972
					1	0.5516448	2.0246790
					2	0.4659101	2.8355408

Fig. 2 reprints the effects of thermal (λ_1) and mass buoyancy parameters (λ_2) on velocity distribution $f'(\eta)$. It is seen that both the parameters have increasing impact on $f'(\eta)$. Fig. 3 shows the effect of magnetic parameter on $f'(\eta)$ in presence/absence of porous matrix. The velocity of the fluid decreases with an increase in magnetic parameter as well as porosity parameter. Physically, the resistive force known as Lorentz force resists the motion of the fluid in porous as well as in non-porous medium. However, the reverse effect is observed in case of temperature distribution $\theta(\eta)$. The reason for this is that an increase in magnetic parameter causes an increase in electromagnetic force that opposes the fluid motion which in turn brings about the temperature rise leading to thicker thermal boundary layer. From Fig. 4 it is observed that suction parameter declines the momentum boundary layer but enhances the thermal boundary layer in $0 \leq \eta \leq 2.5$ and then increases. Further, the velocity of the fluid decreases and temperature of the fluid increases ($0 \leq \eta \leq 2.5$) with an increasing values of velocity ratio parameter. Careful observation reveals that there is no impact of velocity ratio parameter on temperature profile when $\eta \geq 2.5$. The influences of Prandtl number and thermal radiation parameter on temperature profile is depicted in Fig. 5. The temperature and the thermal boundary layer thickness are reduced for the larger Prandtl number. This is due to larger values of Prandtl number lowers the

thermal diffusivity and consequently, lower thermal diffusivity gives rise to a decrease in temperature and lowers the thermal boundary layer thickness. Further, the temperature profile increases with the increase of thermal radiation parameter, which leads to the enormous heat transfer rate through the fluid and the surface. Fig. 6 shows that power law index (m) enhances the temperature profile whereas power law index (n) decreases it. It is perceived that both thermal and solutal bouancy parameters decline the concentration profile (Fig. 7). Fig. 8 depicts the concentration profile for various values of Schmidt number and power law index (m). It is seen that concentration profile decreases with higher values of Schmidt number (Sc) i.e. heavier species. Physically, Schmidt number (Sc) signifies the ratio of momentum to mass diffusivity. Hence by rising Schmidt number minimum mass diffusivity takes place and consequently, reduces the concentration of the fluid. Moreover, power law index (m) also declines concentration of the fluid.

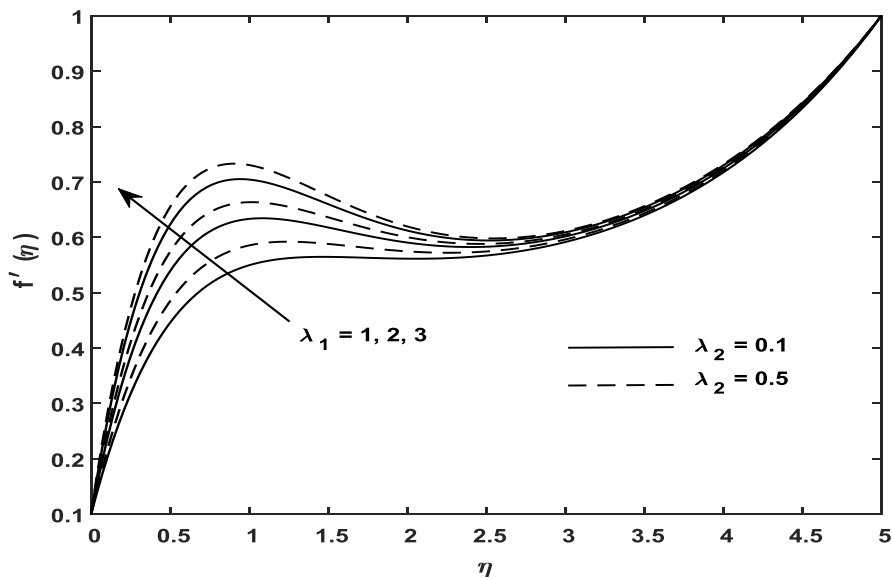


Fig. 2 Velocity profile for various values of λ_1 and λ_2

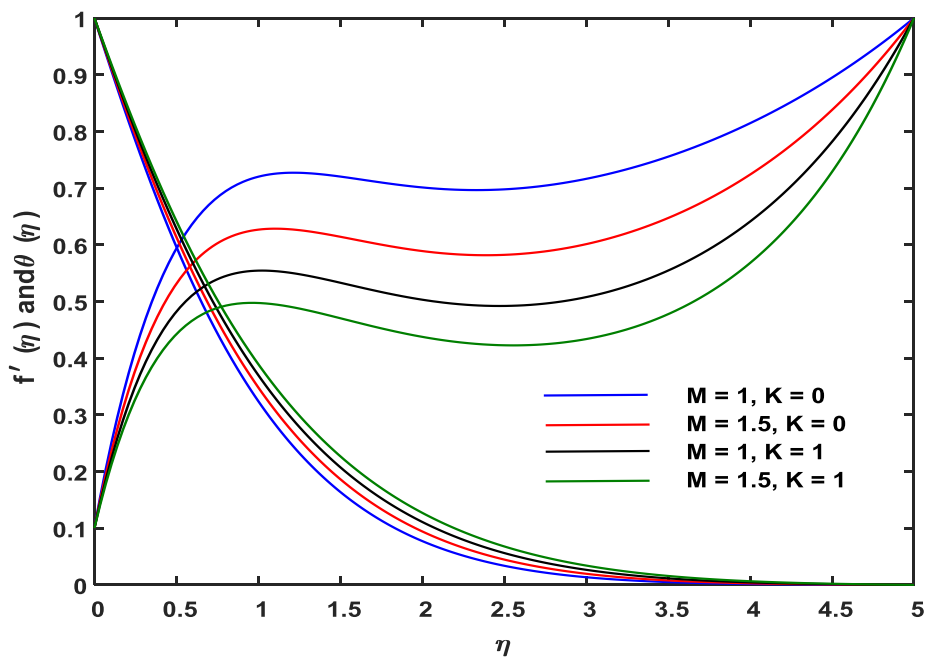


Fig. 3 Velocity and temperature profiles for various values of M and K

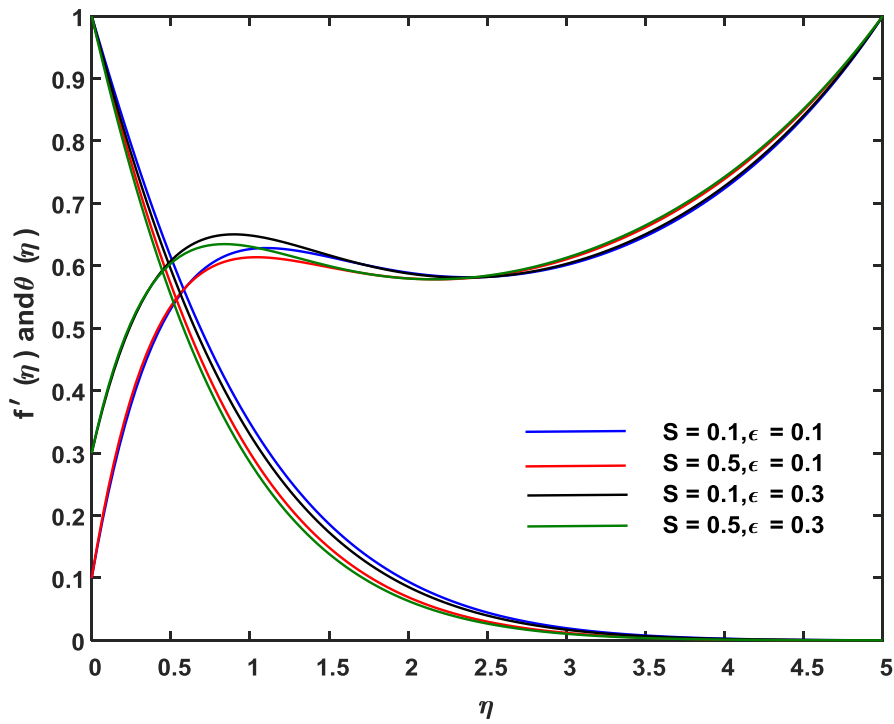


Fig. 4 Velocity and temperature profiles for various values of S and ϵ

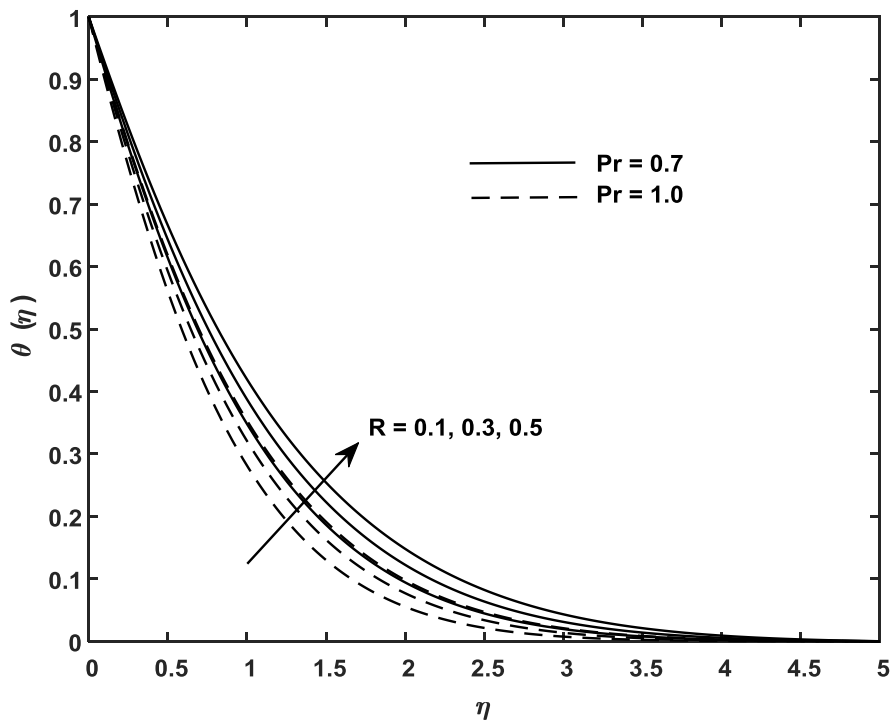


Fig. 5 Temperature profile for various values of Pr and R

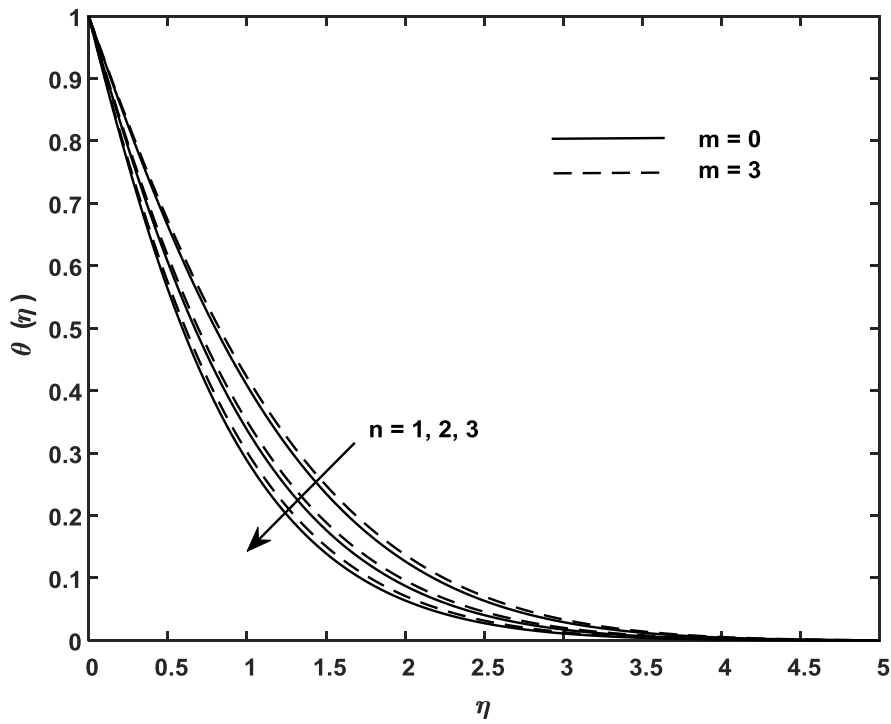


Fig. 6 Temperature profile for various values of m and n

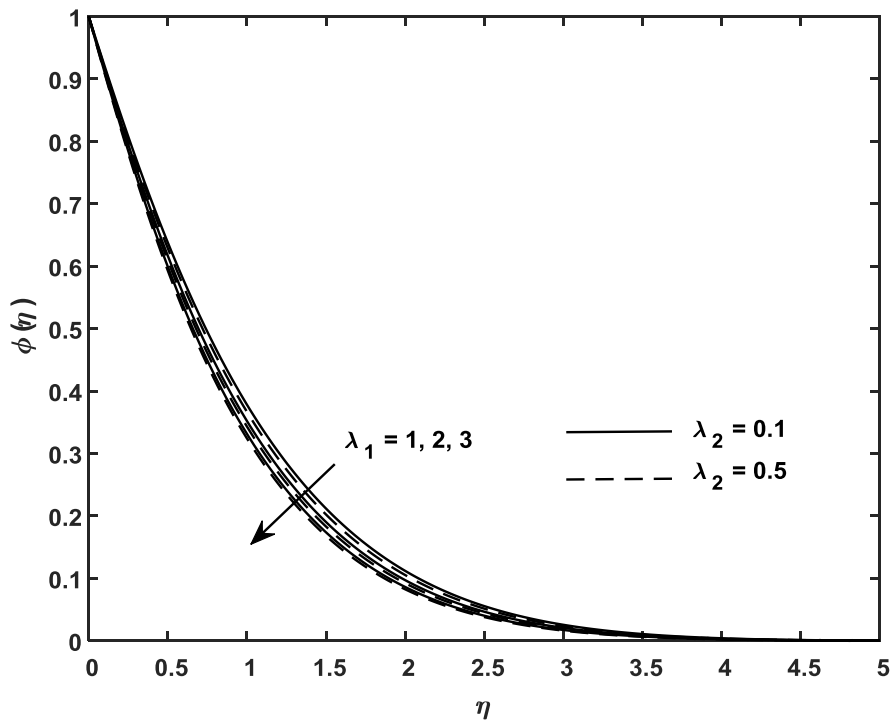


Fig. 7 Temperature profile for various values of λ_1 and λ_2

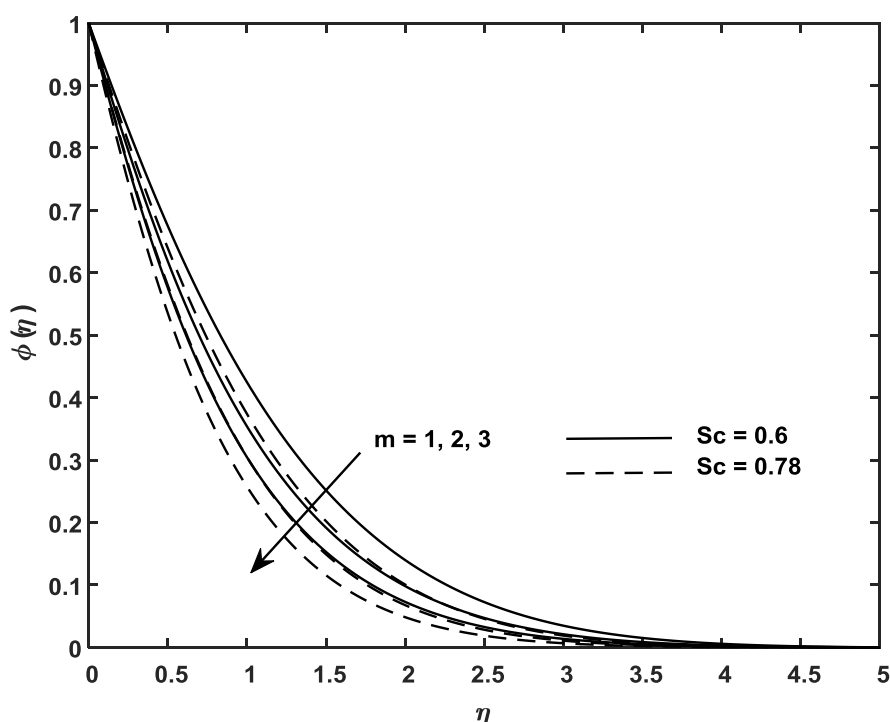


Fig. 8 Concentration profile for various values of Sc and m

V. Concluding remarks

From the present study the following conclusions are drawn:

- Both thermal and solutal bouancy parameters enhance the velocity profile.
- Higher values of radiation parameter and Prandtl number favour the temperature profile.
- Rate of heat transfer declines with an increase in M , R and Sc while enhances with velocity ratio parameter, thermal and solutal buoyancy parameters.
- Concentration profile decreases with higher values of Schmidt number (heavier species).

References

- [1]. L.J. Crane, Flow past a stretching plate, *Z.F. Angew. Math. U. Phys. Zamp*, 21 (4) (1970) 645-647.
- [2]. P.S. Gupta, A.S. Gupta, Heat and mass transfer on a stretching sheet with suction and blowing, *The Canadian Journal of Chemical Engineering*, 55 (6) (1977) 744-746.
- [3]. R. Cortell, Viscous flow and heat transfer over a nonlinearly stretching sheet, *Applied Mathematics and computation*, 184 (2) (2007)864-873.
- [4]. K. Bhattacharya, S. Mukhopadhyay, G. C. Layek, Reactive solute transfer in magneto hydrodynamic boundary layer stagnation-point flow over a stretching sheet with suction/Blowing, *Chemical Engineering Communications*, 199 (3)(2012) 368-383.
- [5]. G.C.Layek, S.Mukhopadhyay,S K.A.Samad, Heat and mass transfer analysis for boundary layer stagnation-point flow towards a heated porous stretching sheet with heat absorption/generation and suction/blowing, *International Communication in Heat and Mass Transfer* 34(3) (2007)347-356
- [6]. K.Bhattacharya, Dual solutions in boundary layer stagnation-point flow and mass transfer with chemical reaction past a stretching/shrinking sheet, *International Communications in Heat and Mass transfer* 38 (7) (2011) 917-922
- [7]. O.D. Makinde, Heat and mass transfer by MHD mixed convection stagnation point flow towards a vertical plate embedded in a highly porous medium with radiation and internal heat generation, *Meccanica* 47 (12)(2012)1173-1184
- [8]. A.Ishak, K.Jafar, R.Najar, I.Pop, MHD stagnation point flow towards a stretching sheet, *Physics A: Statistical Mechanics and its Application* 388 (17)(2009) 3377-3383
- [9]. W.Ibrahim,B.Shankar,M. M. Nandeppanavar, MHD stagnation point flow and heat transfer due to nanofluid towards a stretching sheet, *International Journal of Heat and Mass transfer* 56 (2) (2013) 1-9
- [10]. K. Swain,S.K. Parida,G.C. Dash, MHD heat and mass transfer on stretching sheet with variable fluid properties in porous medium. *Modelling Measurement and control B*, 86(3),(2018)706-726
- [11]. Z. Khan, H.U. Rasheed, S. Islam, S. Noor, W. Khan, T. Abbas, I. Khan, S. Kadry, Y. Nam and K.S. Nisar, Impact of Magneto hydrodynamics on stagnation point slip flow due to nonlinearly propagating sheet with nonuniform thermal reservoir. *Mathematical Problems in Engineering*, Vol 2020, Article ID 1794213, 10 pages.
- [12]. K. Swain, S.K. Parida, G.C. Dash, Effects of non-uniform heat source/sink and viscous dissipation on MHD boundary layer flow of Williamson nanofluid through porous medium, *Defect and Diffusion Forum*, 389 (2018) 110-127.
- [13]. C.Y. Wang, Stagnation flow towards a shrinking sheet, *International Journal of Non-Linear Mechanics* 43 (2008) 377-382.